Lauwers E, Landuyt B, Arckens L, Schoofs L & Luyten W 2006 Obestatin does not activate orphan G protein-coupled receptor GPR39. *Biochemical and Biophysical Research Communications* **351** 21–25.

McKee KK, Tan CP, Palyha OC, Liu J, Feighner SD, Hreniuk DL, Smith RG, Howard AD & Van der Ploeg LH 1997 Cloning and characterization of two human G protein-coupled receptors genes (GPR38 and GPR39) related to the growth hormone secretagogue and neurotensin receptors. *Genomics* **46** 426–434.

Mondal MS, Nakazato M, Date Y, Murakami N, Yanagisawa M & Matsukura S 1999 Widespread distribution of orexin in rat brain and its regulation upon fasting. *Biochemical and Biophysical Research Communications* **256** 495–499.

Nakazato M, Murakami N, Date Y, Kojima M, Matsuo H, Kangawa K & Matsukura S 2001 A role for ghrelin in the central regulation of feeding. *Nature* **409** 194–198.

Nogueiras R, Pfluger P, Tovar S, Arnold M, Mitchell S, Morris A, Perez-Tilve D, Vázquez MJ, Wiedmer P, Castañeda TR *et al.* 2007 Effects of obestatin on energy balance and growth hormone secretion in rodents. *Endocrinology* **148** 21–26.

Ozawa A, Cai Y & Lindberg I 2007 Production of bioactive peptides in an *in vitro* system. *Analytical Biochemistry* **366** 182–189.

Schwartz MW, Woods SC, Porte DJ, Seeley RJ & Baskin DG 2000 Central nervous system control of food intake. *Nature* **404** 661–671.

Shiiya T, Nakazato M, Mizuta M, Date Y, Mondal MS, Tanaka M, Nozoe S, Hosoda H, Kangawa K & Matsukura S 2002 Plasma ghrelin levels in lean and obese humans and the effect of glucose on ghrelin secretion. *Journal of Clinical Endocrinology and Metabolism* **87** 240–244.

de Smet B, Thijs T, Peeters TL & Depoortere I 2007 Effect of peripheral obestatin on gastric emptying and intestinal contractility in rodents. *Neurogastroenterology and Motility* **19** 211–217.

Tack J, Depoortere I, Bisschops R, Verbeke K, Janssens J & Peeters T 2005 Influence of ghrelin on gastric emptying and meal-related symptoms in idiopathic gastroparesis. *Alimentary Pharmacology and Therapeutics* **22** 847–853.

Tschöp M, Smiley DL & Heiman ML 2000 Ghrelin induces adiposity in rodents. *Nature* **407** 908–913.

Tschöp M, Weyer C, Tataranni PA, Devanarayan V, Ravussin E & Heiman ML 2001 Circulating ghrelin levels are decreased in human obesity. *Diabetes* **50** 707–709.

Wren AM, Small CJ, Ward HL, Murphy KG, Dakin CL, Taheri S, Kennedy AR, Roberts GH, Morgan DG, Ghatei MA *et al.* 2000 The novel hypothalamic peptide ghrelin stimulates food intake and growth hormone secretion. *Endocrinology* **141** 4325–4328.

Zhang JV, Ren PG, Avsian-Kretchmer O, Luo CW, Rauch R, Klein C & Hsueh AJ 2005 Obestatin, a peptide encoded by the ghrelin gene, opposes ghrelin's effects on food intake. *Science* **310** 996–999.

Received in final form 30 April 2008
Accepted 14 May 2008
Made available online as an Accepted Preprint
14 May 2008

Available online at www.sciencedirect.com
ScienceDirect
Neuroscience Letters 433 (2008) 38–42
Neuroscience Letters
www.elsevier.com/locate/neulet

The vagal afferent pathway does not play a major role in the induction of satiety by intestinal fatty acid in rats

Nobuya Ogawa [a,b], Hideki Yamaguchi [a], Takuya Shimbara [a], Koji Toshinai [a], Makoto Kakutani [b], Fumihiko Yonemori [b], Masamitsu Nakazato [a,*]

[a] *Division of Neurology, Respirology, Endocrinology and Metabolism, Department of Internal Medicine, Miyazaki Medical College, University of Miyazaki, Kiyotake, Miyazaki 889-1692, Japan*
[b] *Central Pharmaceutical Research Institute, Japan Tobacco, Osaka, Japan*

Received 12 October 2007; received in revised form 18 December 2007; accepted 19 December 2007

Abstract

Intestinal infusion of long-chain fatty acids (LCFAs) strongly suppresses food intake and gut motility. Vagal afferents and cholecystokinin (CCK) signaling pathway are considered to play important roles in intestinal LCFA-induced satiety. Here, we first investigated the influence of vagus nerve on satiety following intestinal LCFA infusion in rats. Jejunal infusion of linoleic acid (LA) at 200 μL/h for 7 h suppressed food intake and the effect lasted for 24 h. The satiety induced by jejunal LA infusion occurred in a dose dependent manner. In contrast, the anorectic effect induced by octanoic acid, a medium-chain fatty acid, was weaker than that induced by LA. The reduction in food intake induced by jejunal LA infusion was not attenuated in rats treated with vagotomy, the ablation of bilateral subdiaphragmatic vagal trunks. Jejunal LA-induced satiety could also be observed in rats with bilateral midbrain transections, which ablates fibers between the hindbrain and hypothalamus. These findings suggest that the vagus nerve and fibers ascending from the hindbrain to the hypothalamus do not play a major role in intestinal LCFA-induced satiety. Jejunal LA infusion also reduced food intake in CCK-A receptor-deficient OLETF rats, suggesting that CCK signaling pathway is not critical for intestinal LCFA-induced anorexia. In conclusion, this study indicates that the vagus nerve and the CCK signaling pathway do not play major roles in conveying satiety signals induced by intestinal LCFA to the brain in rats.

Keywords: Satiety; Fatty acid; Vagotomy; Midbrain transection; CCK-A receptor

Following ingestion of a meal, nutrients and their metabolites begin to modulate short- and long-term food intake, thus regulating energy balance and body weight. Macronutrients in the small intestine induce a range of physiological changes in appetite, gut motility and gut hormone secretion [5,20,25]. Arrival of ingested fat in the small intestine inhibits gastric emptying and gut motility [3,17] and prompts the releases of gut hormones, such as cholecystokinin (CCK), glucagon-like peptide-1 (GLP-1) and peptide YY (PYY) [12,18,19]. These hormones transmit satiety signals [5,20,24] and reduce food intake [27]. Fat digestion, which produces fatty acids, is necessary for the gastrointestinal perception and satiety induction [12,13]. Long-chain fatty acid (LCFA) infusion into the small intestine significantly inhibit food intake in multiple species [4,16,21,29]. Gastrointestinal endocrine cells interact with the factors derived from digested foods at the luminal membrane and in response release gut peptides from the basolateral surface [8]. These peptides diffuse locally to activate nearby vagal afferent fibers from nodose and dorsal root ganglia neurons and enter the blood stream to act on the brain as hormones [8].

The mechanism by which LCFA induces satiety remains unclear. Intestinal fat is thought to induce satiety via the afferent vagal nerve and CCK signaling pathway. In rats, the suppression of food intake that occurs in response to intestinal LCFA could be partially reversed by vagal denervation [6]. Direct electrophysiological recordings of rat vagal afferent fibers demonstrated that intestinal LCFA stimulates neural activity [24], supporting a role for the vagal afferent pathway in intestinal LCFA-induced satiety. Intestinal LCFA triggers the release of anorectic hormones [12,18,19], which transmit signals to the central nervous system via the vagal afferent nerve and/or through the bloodstream. A CCK-A receptor antagonist reversed the intestinal

* Corresponding author. Tel.: +81 985 85 2965; fax: +81 985 85 1869.
E-mail address: nakazato@med.miyazaki-u.ac.jp (M. Nakazato).

0304-3940/$ – see front matter © 2007 Elsevier Ireland Ltd. All rights reserved.
doi:10.1016/j.neulet.2007.12.036

LCFA-induced suppression of food intake in humans [21]; but had little impact on the satiety produced by duodenal oleic acid infusion in rats [28]. Subdiaphragmatic vagotomy or midbrain transection severing ascending fibers of the nucleus of the solitary tract (NTS) can also block CCK-induced reductions in food intake, indicating that CCK transmits satiety signals to the hypothalamus via the afferent limb of the vagus nerve [7,26]. It remains unclear the extent to which the vagal afferent and CCK signaling pathways are involved in intestinal LCFA-induced satiety.

Visceral sensory information is transmitted to the NTS via the vagal afferent nerve. Ascending projections of the NTS contain fibers reaching the ventrolateral and dorsolateral tegmental areas of the hypothalamus, including the dorsal and ventral bundles of catecholaminergic neurons [3]. Both bilateral midbrain transections and subdiaphragmatic bilateral vagotomy are useful to determine the neuronal pathways necessary in the feedback pathway mediating the effects on feeding behaviors of substances produced in peripheral tissues. In this study, we investigated the effect of subdiaphragmatic bilateral vagotomy and bilateral midbrain transections on the anorectic effects induced by jejunal linoleic acid (LA) infusion. We also examined LA-induced satiety in CCK-A receptor-deficient Otsuka Long Evans Tokushima Fatty (OLETF) rats to evaluate the role of the CCK signaling pathway in intestinal LA-induced satiety.

Male Sprague-Dawley rats (Charles River Japan Inc., Shiga, Japan) weighing 300–400 g at surgery, and OLETF rats (the generous gift of Otsuka Pharmaceuticals Research Institute, Tokushima, Japan) weighing 350–400 g at surgery were housed individually in cages under controlled temperature (21–23 °C) and light conditions (light on 08:00–20:00) with *ad libitum* access to food and water. All procedures were performed in accordance with the Japanese Physiological Society's guidelines for animal care. Prior to surgery, the rats fasted overnight. Animals were anesthetized with intraperitoneal 50 mg/kg pentobarbital sodium (Abbott Laboratories, Chicago, IL). After abdominal celiotomy, we inserted a polyethylene tube (SP28; I.D. 0.4 mm O.D. 0.8 mm, Natsume, Tokyo, Japan) into the duodenum 5 cm from the pylorus. The end of the tube reached the proximal jejunum 10 cm from the pylorus. The tube was fixed to the entrance of the intestine with silk sutures. The opposite end of the tube was threaded through the opening in the abdominal wall and tunneled subcutaneously to the dorsal surface of the neck, where a Dacron mesh anchor button (DC95, Instech Solomon, Plymouth Meeting, PA) was implanted. The tube was also fixed to the ventral abdominal wall and the anchor button mesh using silk sutures. After a 1–2 week recovery period, rats had become adapted enough to the continuous infusion apparatus (Instech Solomon) to allow us to perform a series of experiments.

In our feeding tests, 1 h before onset of the dark phase (19:00), food was removed from the cage. We then began jejunal infusion of linoleic acid (commercial grade, ~60% linoleic acid, ~30% oleic acid, Sigma, St. Louis, MO), octanoic acid (minimum 99%, Sigma) or saline. At the onset of the dark phase (20:00), we restarted feeding. Infusion lasted for 7 h (19:00–02:00) or 4 h (19:00–23:00); cumulative food intake was measured for 23 h or 3 h, respectively. All experiments were conducted using crossover methods, in which all animals received jejunal infusion of fatty acids or saline on separate days. All data are expressed as means ± S.D. Groups of data were compared using the Student's *t*-test and Dunnett test. *P*-values less than 0.05 were considered significant.

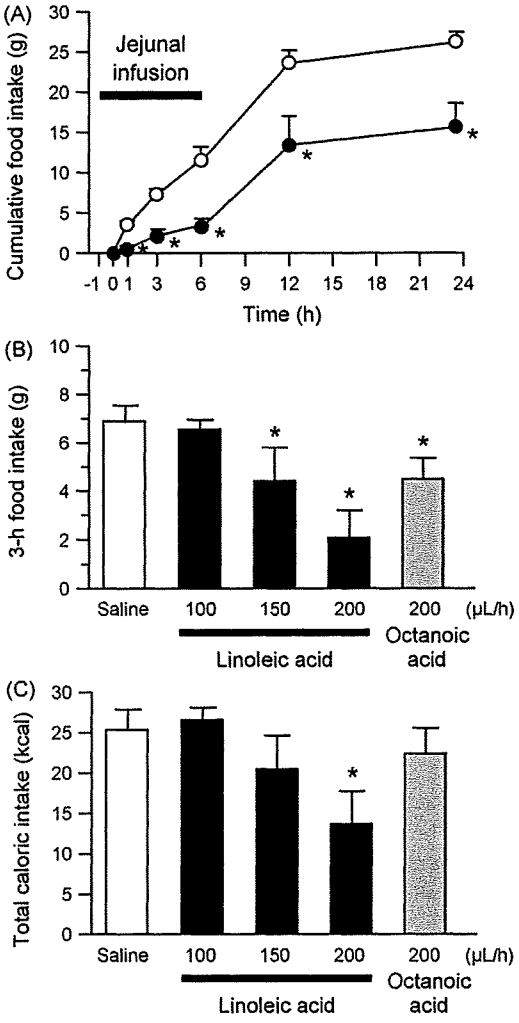

Fig. 1. Jejunal fatty acid infusion reduced food intake in rats. (A) Cumulative food intake in rats after jejunal infusion of linoleic acid or saline at 200 μL/h for 7 h. *$P < 0.01$ vs. saline group: $n = 6$/group. (B) Three hour food intake in rats after jejunal infusion of linoleic acid, octanoic acid or saline for 4 h at a variety of infusion rates. *$P < 0.01$ vs. saline group: $n = 6$/group. (C) Total caloric intake in rats after jejunal infusion of linoleic acid, octanoic acid or saline for 4 h at a variety of infusion rates. *$P < 0.01$ vs. saline group: $n = 6$/group.

The 7-h jejunal infusion of LA at 200 μL/h significantly reduced food intake at all time points (Fig. 1A) by approximately 40%. The cumulative food intake for 23 h for the saline group was 26.35 ± 1.49 g, while that for LA-treated group was 15.94 ± 2.85 g ($P < 0.01$). The induction of satiety following a 4-h jejunal LA infusion was dependent on infusion rate (Fig. 1B), with a lowest effective dose of 150 μL/h. Infusion of 200 μL/h octanoic acid (OA), a middle chain fatty acid (MCFA), also reduced food intake (Fig. 1B) with a weaker efficacy than that of LA infusion (3-h food intake: saline group; 6.97 ± 0.76 g, LA 100 μL/h group; 6.57 ± 0.45 g, LA 150 μL/h group; 4.38 ± 1.37 g, $P < 0.01$, LA 200 μL/h group;

2.01 ± 1.13 g, $P < 0.01$, OA 200 μL/h group; 4.46 ± 0.84 g, $P < 0.01$). When we calculate the total caloric intake from food intake and infused fatty acids, jejunal infusion of LA, but not OA, reduced the total caloric intake of rats (3-h calorie intake: saline group; 25.04 ± 2.73 kcal, LA 100 μL/h group; 26.82 ± 1.60 kcal, LA 150 μL/h group; 20.57 ± 4.91 kcal, LA 200 μL/h group; 13.70 ± 4.06 kcal, $P < 0.01$, OA 200 μL/h group; 22.49 ± 3.03 kcal) (Fig. 1C). We also examined the effect of oleic acid (minimum 95%, Sigma) to confirm the validity of our experimental system. We obtained the comparable result to LA infusion (3-h food intake: saline group; 6.75 ± 0.48 g, oleic acid 200 μL/h group; 2.18 ± 0.33 g, $P < 0.01$, $n = 4$). These findings are consistent with previous results that intestinal fatty acids suppress food intake in a manner dependent on the chain length of fatty acids [9,19]. Previous studies in humans have demonstrated that fat digestion is necessary for the suppression of appetite, gastrointestinal motility, and hormone secretion [12,13]; the chain length of fatty acids is important for these effects [14].

Next, we investigated the effect of the gut–brain neuronal pathway on jejunal LCFA-induced satiety using truncal vagotomized rats and bilateral midbrain-transectioned rats. The vagus nerve, which is composed of a number of branches, transmits afferent and efferent signals to and from abdominal organs. Approximately, 90% of vagal nerve fibers in the subdiaphragm are afferent, unmyelinated fibers [1]. Several gut hormones, including CCK and ghrelin, transmit their appetite-modulating signals via the vagal afferent pathway [9,26]. Peripheral metabolic signals are then relayed by the ascending efferent fibers of the NTS to the hypothalamus [7,10]. However, recent evidence shows that ghrelin effect on food intake is vagal independent [2]. Intestinal nutrients, both carbohydrates and fats, lead to both the release of gut hormones, such as CCK, GLP-1 and PYY, and the activation of vagal afferent fibers. Although it is theoretically possible that the vagus nerve directly senses nutrients in the lumen of the intestine, it has been clearly established that gut hormones released from enteroendocrine cells mediate neural activation [8]. We therefore expected the involvement of the vagal afferent nerve in the suppression of food intake induced by intestinal fatty acid infusion.

Subdiaphragmatic bilateral vagotomy was performed as described [26] prior to intra-jejunal cannulation. After exposure of the bilateral subdiaphragmatic trunks of the vagus nerve along the esophagus [1], we excised trunk sections at least 0.5 cm in length. To validate the vagotomy, we confirmed that intraperitoneal administration of CCK did not induce an anorectic effect in vagotomized rats [4,26]. Jejunal LA infusion at 200 μL/h reduced food intake in both sham-operated rats and truncal vagotomized rats (3-h food intake: sham-saline group; 7.07 ± 0.61 g, sham-LA group; 2.03 ± 1.27 g, $P < 0.01$ vs. sham-saline group, vagotomy-saline group; 6.20 ± 0.83 g, vagotomy-LA group; 2.19 ± 1.51 g, $P < 0.01$ vs. vagotomy-saline group) (Fig. 2). While CCK administration (5 nmol/rat) reduced 1-h food intake in sham-operated rats, the anorectic effects of CCK could not be observed in vagotomized rats (1-h food intake: sham-vehicle group; 3.23 ± 0.22 g, sham-CCK group; 1.42 ± 0.20 g, $P < 0.01$ vs. sham-vehicle group, vagotomy-vehicle group; 2.33 ± 0.50 g, vagotomy-CCK group; 2.15 ± 0.41 g, $n = 3$).

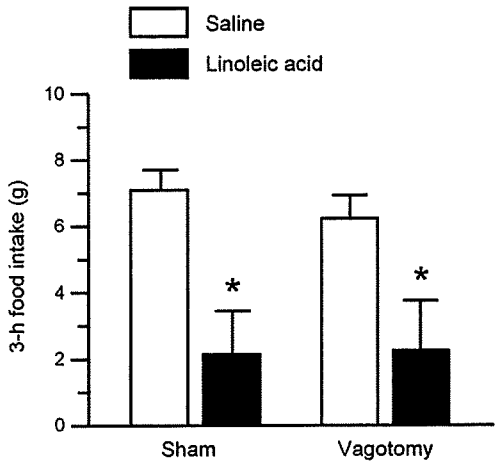

Fig. 2. Subdiaphragmatic bilateral vagotomy did not attenuate the satiety induced by jejunal linoleic acid infusion. Three hour food intake in sham-operated and truncal vagotomized rats after jejunal infusion of linoleic acid or saline at 200 μL/h for 4 h. *$P < 0.01$ vs. saline group: $n = 3$/group (sham-operated rats), $n = 6$/group (truncal vagotomized rats).

Cox et al. showed that the reduction in food intake induced by jejunal LA infusion was due to the contribution of vagus nerve. However, jejunal lipid infusions still reduced food intake approximately half as much effectively as in control animals even after truncal vagotomy, revealing the substantial involvement of a mechanism independent of the vagal pathway. Phifer and Berthoud [23] reported that intestinal fatty acid infusion increased cFos expression, a marker of neuronal activation, in the NTS in rats. These results suggested that intestinal LCFA signals satiety via neural and humoral pathways. Visceral information is transmitted to the NTS in the hindbrain via the vagal afferent nerve. Ascending projections of the NTS relay and transfer the information to the ventrolateral and dorsolateral tegmental areas of the hypothalamus. To investigate the involvement of the neural pathway in intestinal LCFA-induced satiety, we examined the anorectic effects induced by intestinal LCFA in rats with bilateral midbrain transections that ablated the fibers between the hindbrain and the hypothalamus.

Bilateral midbrain transection was performed as described [7] prior to the intra-jejunal cannulation. The heads of experimental animals were fixed in a stereotaxic instrument in a 2.4 mm nose-down position. We inserted a 1.5 mm-wide razor into the brain bilaterally in a coronal plane, 0.5 mm from the midline, 1 mm anterior to the lambdoidal suture, and 7.7 mm ventral to the dura. To validate the efficacy of the midbrain transection surgery, we confirmed that the procedure abrogated the anorectic effect induced by intraperitoneal administration of CCK in transectioned rats [7]. Brains were removed after feeding testing; we then verified the exact location of the lesions histologically and identified the sectioned noradrenergic fibers by immunostaining using an anti-dopamine β hydroxylase (DBH) antiserum (1:1000, Chemicon international Inc., Temecula, CA) using the avidin–biotin complex method [11]. Jejunal LA infusion strongly reduced food intake

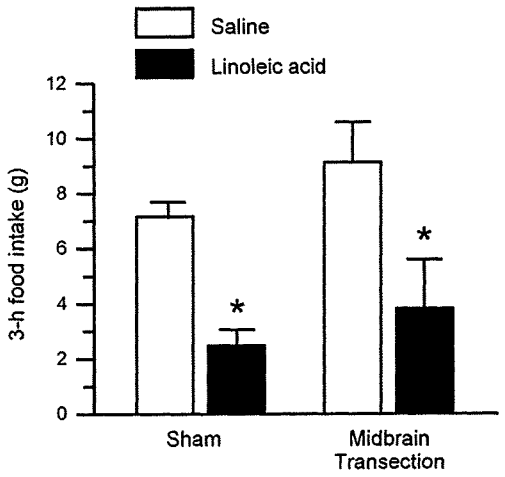

Fig. 3. Bilateral midbrain-transections did not affect the satiety induced by jejunal linoleic acid infusion. Three hour food intake in bilateral midbrain-transectioned rats after jejunal infusion of linoleic acid or saline at 200 μL/h for 4 h. *$P < 0.01$ vs. saline group: $n = 3$/group (sham-operated rats), $n = 6$/group (midbrain-transectioned rats).

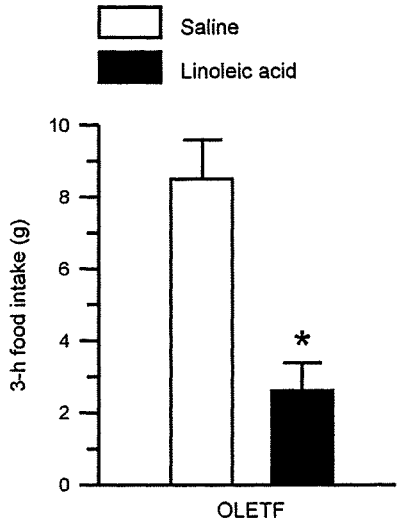

Fig. 4. Effect of CCK-A signaling on the satiety induced by jejunal linoleic acid infusion. Three hour food intake in CCK-A receptor-deficient OLETF rats after jejunal infusion of linoleic acid or saline at 200 μL/h for 4 h. *$P < 0.01$ vs. saline group: $n = 3$/group.

in both sham-operated rats and midbrain-transectioned rats (3-h food intake: sham-saline group; 7.10 ± 0.60 g, sham-LA group; 2.50 ± 0.80 g, $P < 0.01$ vs. sham-saline group, transection-saline group; 9.04 ± 1.57 g, transection-LA group; 3.93 ± 1.93 g, $P < 0.01$ vs. transection-saline group) (Fig. 3). Similarly to the results seen in vagotomized rats, the anorectic effects of CCK (5 nmol/rat i.p.) were not observed in midbrain-transectioned rats (1-h food intake: sham-vehicle group; 3.01 ± 0.31 g, sham-CCK group; 1.10 ± 0.28 g, $P < 0.01$ vs. sham-vehicle group, transection-vehicle group; 3.92 ± 0.54 g, transection-CCK group; 3.75 ± 0.58 g, $n = 3$). After completion of feeding tests, we verified the dissection of noradrenergic fibers by DBH immunostaining (data not shown). Although we have not conducted the capsaicin experiment to confirm the importance of vagal afferent pathway, our findings suggested that neither truncal vagotomy nor midbrain transection affected the suppression of food intake induced by intestinal LA infusion. These results indicated that the vagal afferent pathway did not play a major role in intestinal LA-induced satiety.

CCK is an intestinal anorectic peptide that is produced and secreted by enteroendocrine cells in response to luminal nutrients [15]. Biologically active CCK interacts with two receptors, CCK-A and -B receptors, which are expressed in the gut and brain. In the vagal afferent pathway, the CCK-A receptor mediates CCK-induced satiety [22,26]. CCK-A receptor-deficient OLETF rats exhibited increased food intake and mild obesity [22]. To examine the involvement of CCK signaling in LCFA-induced satiety, we investigated the anorectic effect of intestinal LCFA in CCK-A receptor-deficient OLETF rats. Jejunal infusion of LA at 200 μL/h significantly reduced food intake in OLETF rats (Fig. 4). The 3-h food intake for the saline group was 8.50 ± 1.18 g, while that for LA-treated group was 2.67 ± 0.78 g ($P < 0.01$). The efficacy of intestinal LCFA-induced food intake reduction in OLETF rats was comparable to that observed in normal rats. Brenner et al. reported that the suppression of sham feeding by intraintestinal nutrients was not correlated with plasma level of CCK [4]. These findings suggested that CCK signaling pathway did not play a major role in the intestinal LCFA-induced suppression of food intake in rats. Several lines of evidence indicated that intestinal fat stimulated the secretion of multiple gut hormones, lead us to explore whether GLP-1, anorectic gut hormone, is involved in intestinal fat-induced satiety [12,18,19]. GLP-1 is a gut hormone secreted from enteroendocrine L cells in response to ingested nutrients and suppresses food intake and gut motility. We measured the plasma level of GLP-1 using a GLP-1 ELISA kit (Wako Pure Chemical, Osaka, Japan). Jejunal LA significantly increased the plasma level of GLP-1 (saline group; 0.96 ± 0.09 ng/mL, LA group; 2.07 ± 0.46 ng/mL, $P < 0.05$, $n = 3$). These results suggested that GLP-1 might partly be involved in the transmission of satiety signal to hypothalamus directly through the bloodstream.

In conclusion, we demonstrated that jejunal infusion of LCFA, but not MCFA, reduced food intake in rats. The suppression of food intake induced by jejunal LCFA was unaffected by subdiaphragmatic bilateral vagotomy or bilateral midbrain transection. Jejunal LCFA infusion retained the ability to induce satiety in OLETF rats. These results indicate that the vagal afferent pathway and CCK-A receptor signaling pathway do not play essential roles in the intestinal LCFA-induced suppression of feeding behavior in rats.

Acknowledgement

This study was supported in part by Society of Molecular Mechanism of Digestive Tract (M.N.)

References

[1] E. Agostoni, J.E. Chinnock, M.B. De Daly, J.G. Murray, Functional and histological studies of the vagus nerve and its branches to the heart, lungs and abdominal viscera in the cat, J. Physiol. 135 (1957) 182–205.

[2] M. Arnold, A. Mura, W. Langhans, N. Geary, Gut vagal afferents are not necessary for the eating-stimulatory effect of intraperitoneally injected ghrelin in the rat, J. Neurosci. 26 (2006) 11052–11060.
[3] F. Azpiroz, J.R. Malagelada, Intestinal control of gastric tone, Am. J. Physiol. 249 (1985) G501–G509.
[4] L. Brenner, D.P. Yox, R.C. Ritter, Suppression of sham feeding by intraintestinal nutrients is not correlated with plasma cholecystokinin elevation, Am. J. Physiol. 264 (1993) R972–R976.
[5] I.M. Chapman, E.A. Goble, G.A. Wittert, M. Horowitz, Effects of small-intestinal fat and carbohydrate infusions on appetite and food intake in obese and nonobese men, Am. J. Clin. Nutr. 69 (1999) 6–12.
[6] J.E. Cox, G.R. Kelm, S.T. Meller, A. Randich, Suppression of food intake by GI fatty acid infusions: roles of celiac vagal afferents and cholecystokinin, Physiol. Behav. 82 (2004) 27–33.
[7] J.N. Crawley, J.Z. Kiss, E. Mezey, Bilateral midbrain transections block the behavioral effects of cholecystokinin on feeding and exploration in rats, Brain Res. 322 (1984) 316–321.
[8] D.E. Cummings, J. Overduin, Gastrointestinal regulation of food intake, J. Clin. Invest. 117 (2007) 13–23.
[9] Y. Date, N. Murakami, K. Toshinai, S. Matsukura, A. Niijima, H. Matsuo, K. Kangawa, M. Nakazato, The role of the gastric afferent vagal nerve in ghrelin-induced feeding and growth hormone secretion in rats, Gastroenterology 123 (2002) 1120–1128.
[10] Y. Date, T. Shimbara, S. Koda, K. Toshinai, T. Ida, N. Murakami, M. Miyazato, K. Kokame, Y. Ishizuka, Y. Ishida, H. Kageyama, S. Shioda, K. Kangawa, M. Nakazato, Peripheral ghrelin transmits orexigenic signals through the noradrenergic pathway from the hindbrain to the hypothalamus, Cell Metab. 4 (2006) 323–331.
[11] Y. Date, Y. Ueta, H. Yamashita, H. Yamaguchi, S. Matsukura, K. Kangawa, T. Sakurai, M. Yanagisawa, M. Nakazato, Orexins, orexigenic hypothalamic peptides, interact with autonomic, neuroendocrine and neuroregulatory systems, Proc. Natl. Acad. Sci. USA 96 (1999) 748–753.
[12] C. Feinle, D. O'Donovan, S. Doran, J.M. Andrews, J. Wishart, I. Chapman, M. Horowitz, Effects of fat digestion on appetite, APD motility, and gut hormones in response to duodenal fat infusion in humans, Am. J. Physiol. Gastrointest. Liver Physiol. 284 (2003) G798–G807.
[13] C. Feinle, T. Rades, B. Otto, M. Fried, Fat digestion modulates gastrointestinal sensations induced by gastric distention and duodenal lipid in humans, Gastroenterology 120 (2001) 1100–1107.
[14] K.L. Feltrin, T.J. Little, J.H. Meyer, M. Horowitz, A.J. Smout, J. Wishart, A.N. Pilichiewicz, T. Rades, I.M. Chapman, C. Feinle-Bisset, Effects of intraduodenal fatty acids on appetite, antropyloroduodenal motility, and plasma CCK and GLP-1 in humans vary with their chain length, Am. J. Physiol. Regul. Integr. Comp. Physiol. 287 (2004) R524–R533.
[15] J. Gibbs, R.C. Young, G.P. Smith, Cholecystokinin elicits satiety in rats with open gastric fistulas, Nature 245 (1973) 323–325.
[16] P.C. Gregory, D.V. Rayner, The influence of gastrointestinal infusion of fats on regulation of food intake in pigs, J. Physiol. 385 (1987) 471–481.
[17] R. Heddle, J. Dent, N.W. Read, L.A. Houghton, J. Toouli, M. Horowitz, G.J. Maddern, J. Downton, Antropyloroduodenal motor responses to intraduodenal lipid infusion in healthy volunteers, Am. J. Physiol. 254 (1988) G671–G679.
[18] P. Lilja, I. Wiener, K. Inoue, G.M. Fried, G.H. Greeley Jr., J.C. Thompson, Release of cholecystokinin in response to food and intraduodenal fat in pigs, dogs and man, Surg. Gynecol. Obstet. 159 (1984) 557–561.
[19] H.C. Lin, W.Y. Chey, Cholecystokinin, peptide, YY are released by fat in either proximal or distal small intestine in dogs, Regul. Pept. 114 (2003) 131–135.
[20] C.G. MacIntosh, M. Horowitz, M.A. Verhagen, A.J. Smout, J. Wishart, H. Morris, E. Goble, J.E. Morley, I.M. Chapman, Effect of small intestinal nutrient infusion on appetite, gastrointestinal hormone release, and gastric myoelectrical activity in young and older men, Am. J. Gastroenterol. 96 (2001) 997–1007.
[21] D. Matzinger, L. Degen, J. Drewe, J. Meuli, R. Duebendorfer, N. Ruckstuhl, M. D'Amato, L. Rovati, C. Beglinger, The role of long chain fatty acids in regulating food intake and cholecystokinin release in humans, Gut 46 (2000) 688–693.
[22] T.H. Moran, L.F. Katz, C.R. Plata-Salaman, G.J. Schwartz, Disordered food intake and obesity in rats lacking cholecystokinin A receptors, Am. J. Physiol. 274 (1998) R618–R625.
[23] C.B. Phifer, H.R. Berthoud, Duodenal nutrient infusions differentially affect sham feeding and Fos expression in rat brain stem, Am. J. Physiol. 274 (1998) R1725–R1733.
[24] A. Randich, W.J. Tyler, J.E. Cox, S.T. Meller, G.R. Kelm, S.S. Bharaj, Responses of celiac and cervical vagal afferents to infusions of lipids in the jejunum or ileum of the rat, Am. J. Physiol. Regul. Integr. Comp. Physiol. 278 (2000) R34–R43.
[25] R.C. Ritter, Gastrointestinal mechanisms of satiation for food, Physiol. Behav. 81 (2004) 249–273.
[26] G.P. Smith, C. Jerome, B.J. Cushin, R. Eterno, K.J. Simansky, Abdominal vagotomy blocks the satiety effect of cholecystokinin in the rat, Science 213 (1981) 1036–1037.
[27] I.M. Welch, C.P. Sepple, N.W. Read, Comparisons of the effects on satiety and eating behaviour of infusion of lipid into the different regions of the small intestine, Gut 29 (1988) 306–311.
[28] T. Woltman, D. Castellanos, R. Reidelberger, Role of cholecystokinin in the anorexia produced by duodenal delivery of oleic acid in rats, Am. J. Physiol. 269 (1995) R1420–R1433.
[29] T. Woltman, R. Reidelberger, Effects of duodenal and distal ileal infusions of glucose and oleic acid on meal patterns in rats, Am. J. Physiol. 269 (1995) R7–R14.

Available online at www.sciencedirect.com
ScienceDirect
Regulatory Peptides 145 (2008) 141 – 146
REGULATORY PEPTIDES
www.elsevier.com/locate/regpep

Ontogeny of a new enteric peptide, neuropeptide W (NPW), in the developing rat stomach

Muhtashan S. Mondal [a], Hideki Yamaguchi [a], Yukari Date [a], Tomoko Tsuruta [a], Takuya Shimbara [a], Koji Toshinai [a], Yukio Shimomura [b], Masaaki Mori [c], Masamitsu Nakazato [a,*]

[a] *Division of Neurology, Respirology, Endocrinology, and Metabolism, Department of Internal Medicine, Faculty of Medicine, University of Miyazaki, Kiyotake, Miyazaki 889-1692, Japan*
[b] *Frontier Research Laboratories, Pharmaceutical Research Division, Takeda Pharmaceutical Company Limited, Tsukuba, Ibaraki 300-4293, Japan*
[c] *Pharmacology Research Laboratories I, Pharmaceutical Research Division, Takeda Pharmaceutical Company Limited, Osaka 532-8686, Japan*

Available online 26 September 2007

Abstract

Neuropeptide W (NPW), a novel endogenous peptide for G protein-coupled receptors GPR7 and GPR8, is expressed in the gastric antral mucosa of rat, mouse, and human stomachs. Here, we studied the ontogeny of NPW in the developing rat stomach. Real-time RT-PCR showed that NPW gene expression was initially detectable in embryonic day 14 (E14) stomach and gradually increased during the progress of age until birth, postnatal day 1 (P1). NPW mRNA level in the stomach increased again from the weaning period (P21) until reaching adulthood. Immunohistochemistry using polyclonal antibodies raised against rat NPW revealed that NPW-positive cells were detected in the P1 antral stomach and gradually increased during the development of age. Furthermore, double immunohistochemistry demonstrated that NPW colocalized with gastrin in P1 rat stomach. These data will provide clues to physiological functions of NPW in the development of rat stomach.

Keywords: NPW; Ontogeny; RT-PCR; Immunohistochemistry; Gastrin

1. Introduction

G protein-coupled receptors (GPCRs), GPR7 and GPR8, are widely expressed in the brain and periphery and have significant similarity with opioid and somatostatin receptors [1]. GPR7 and GPR8 share 70% nucleotide and 64% amino acid identity [1]. GPR7 was highly conserved in both human and rodents, while GPR8 was not found in the rodent genomes [2]. In rat brain, GPR7 mRNA was widely expressed throughout the brain, including the paraventricular, supraoptic, ventromedial hypothalamic, dorsomedial hypothalamic, suprachiasmatic, and arcuate nuclei, areas which are all important for feeding regulation and energy homeostasis [2]. Male GPR7 knockout mice have shown to develop an adult-onset obese phenotype [3].

Neuropeptide W (NPW) was recently isolated from the porcine hypothalamus, using a cAMP accumulation inhibition assay of Chinese hamster ovary cell lines, as an endogenous ligand for GPR7 and GPR8 [4]. NPW homologues have been identified using the porcine cDNA sequence for prepro-NPW in swine, rat, and human cDNA fragments, indicating that NPW is highly conserved among species [4]. Two mature forms of the peptide have been identified, termed NPW23 and NPW30, the former corresponding to a C-terminal truncation of NPW30. Human NPW differs from the rat form by only one amino acid at position 17. Synthetic NPW23 and NPW30 peptides have similar potency to bind and activate GPR7 and GPR8. In the rat brain, NPW-immunoreactive cells were detected in the ventral tegmental area, periaqueductal gray, and Edinger–Westphal nucleus [5]. Centrally administered NPW23 increases serum corticosterone levels and augments water drinking in rats [6]. When centrally administered, both NPW23 and NPW30 suppressed dark-phase and fasting-induced food intake at similar effective doses in rats [7]. Continuous central infusion of NPW23 suppressed feeding and body weight gain over the infusion period. Conversely, central administration of anti-NPW IgG increased food intake. Furthermore, central administration of NPW increased body temperature and heat production. Taken

* Corresponding author. Tel.: +81 985 85 2965; fax: +81 985 85 1869.
E-mail address: nakazato@med.miyazaki-u.ac.jp (M. Nakazato).

0167-0115/$ - see front matter © 2007 Elsevier B.V. All rights reserved.
doi:10.1016/j.regpep.2007.09.029

together, these results indicate that NPW may function as an endogenous catabolic signaling molecule in the brain.

In the periphery, GPR7 and NPW mRNA are robustly expressed in rat stomach [8,9]. We have shown that NPW cells are present in the mucosal layer of the gastric antrum of rat, mouse, and human stomachs [10]. By using double immunohistochemistry and electron microscopic immunohistochemistry, we showed that NPW colocalized with gastrin in the antral gastric cells [10]. In the present study, we characterized the ontogeny of NPW gene expression by real-time reverse-transcription polymerase chain reaction (RT-PCR) and that of NPW-positive cells by immunohistochemistry in the developing rat stomach. We also studied the colocalization of NPW with gastrin in developing rat stomach.

2. Materials and methods

2.1. Animals

Adult timed-pregnant, nursing female and male Wistar rats (Charles River Japan, Inc., Shiga, Japan) were maintained in an air-conditioned (24±2 °C) and light-regulated room (lights on, 0800–2000 h). Animals were given standard laboratory chow and water *ad libitum*. All procedures were performed in accordance with the Japanese Physiological Society's guidelines for animal care. The experimental protocol was approved by the Ethics Review Committee for Animal Experimentation of the Faculty of Medicine, University of Miyazaki.

2.2. Peptide synthesis

Human NPW23 and NPW30, rat NPW23 and NPW30, and [^{14}Cys] human NPW- [1–13] were synthesized using an ABI 433A peptide synthesizer (Applied Biosystems Inc., Foster City, CA) as previously reported [10].

2.3. Preparation and characterization of antisera

Polyclonal anti-NPW antisera recognizing N-terminal of human NPW23 and 30 were raised according to our previous report [10]. The resulting human polyclonal antisera exhibited 100% cross-reactivity with rat NPW23 and NPW30.

2.4. Quantitative TaqMan PCR analysis of NPW expression

Male fetal stomachs and antral portion of the stomachs from pups and adult was used for PCR analysis. Total RNA was extracted from the fetal stomachs at different stages of development (embryonic E14 and E17) from timed-pregnant rats, stomachs of rat pups at different ages (postnatal P1, P7, and P21), and adult rat stomachs using the acid guanidinium thiocyanate-phenol-chloroform (AGPC) method [11]. Total RNA (0.5 μg) was reverse transcribed to cDNA using Superscript III reverse transcriptase (Invitrogen, Carlsbad, CA) with a random primer. NPW mRNA expression was measured by quantitative PCR method using Applied Biosystems 7300 Real-Time PCR system. Rodent GAPDH Control Reagent (Applied Biosystems, Foster City, CA) was purchased and the primers and probe of rat prepro-NPW were synthesized. PCR primers for NPW were 5′-TGGCGTCGAGCAGAGAAGTAC-3′ and 5′-ACCCA CTGTGTGATAGCGAGG-3′, and probe for NPW was 5′-(6-carboxyfluorescein)-CTGCTACCGCTACTGCTGCTTCTG CTC-(6-carboxy-tetramethyl-rhodamine)-3′. The PCR reaction was performed as follows: at 50 °C for 2 min, at 95 °C for 10 min, and 40 cycles at 95 °C for 15 s and at 60 °C for 1 min. Copy number of target gene was calculated based on comparison of the amplification plots between cDNA samples and standards.

2.5. Immunohistochemistry

After stomachs were resected from the fetus of E14 and E17, and antral stomachs from postnatal pups of P1, P7, P21, and adult rats, the samples were post fixed with fixative for 24 h at 4 °C, and then incubated for 24 h in 0.1 M phosphate-buffered saline (PBS, pH 7.4) containing 30% sucrose. Samples were cut serially at −20 °C with a cryostat into slices 7 μm thick, then thaw-mounted on silane-coated slides and stored at −80 °C. Serial sections were treated with 0.3% hydrogen peroxide to inactivate endogenous peroxidase activity, and then incubated with normal goat serum to block non-specific binding. These sections were incubated overnight at 4 °C with anti-NPW- [1–13] antiserum (final dilution 1:5000). We subsequently performed double staining for NPW with polyclonal anti-gastrin antiserum (DAKO Corp., Carpinteria, CA; final dilution 1:5). All sections were stained using the avidin-biotin complex method described previously [12]. We examined three immunostained slides for analytical purposes. Control studies were done with normal rabbit serum or anti-NPW- [1–13] antiserum that had been pre-absorbed with 10 μg rat NPW.

3. Results

3.1. Ontogeny of stomach NPW gene expression

Real-time RT-PCR showed that NPW mRNA transcript was initially detectable in the embryonic day 14 of age stomach (Fig. 1). From E14 day of age, stomach NPW mRNA increased progressively as function of age through day of birth, postnatal

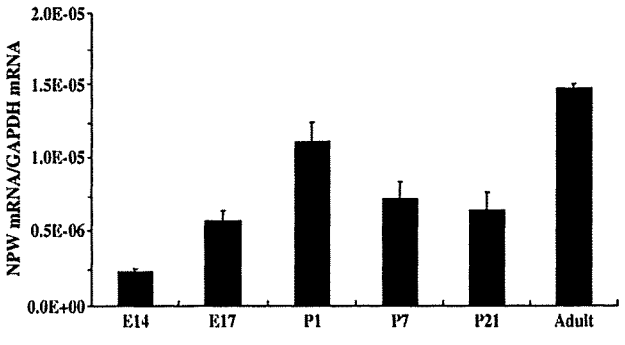

Fig. 1. The relative levels of NPW mRNA transcripts in the developing rat stomach. The relative expression of NPW mRNA transcripts was expressed relative to the GAPDH signal in the same PCR analysis. Values are mean ± S.E., $n=5$.

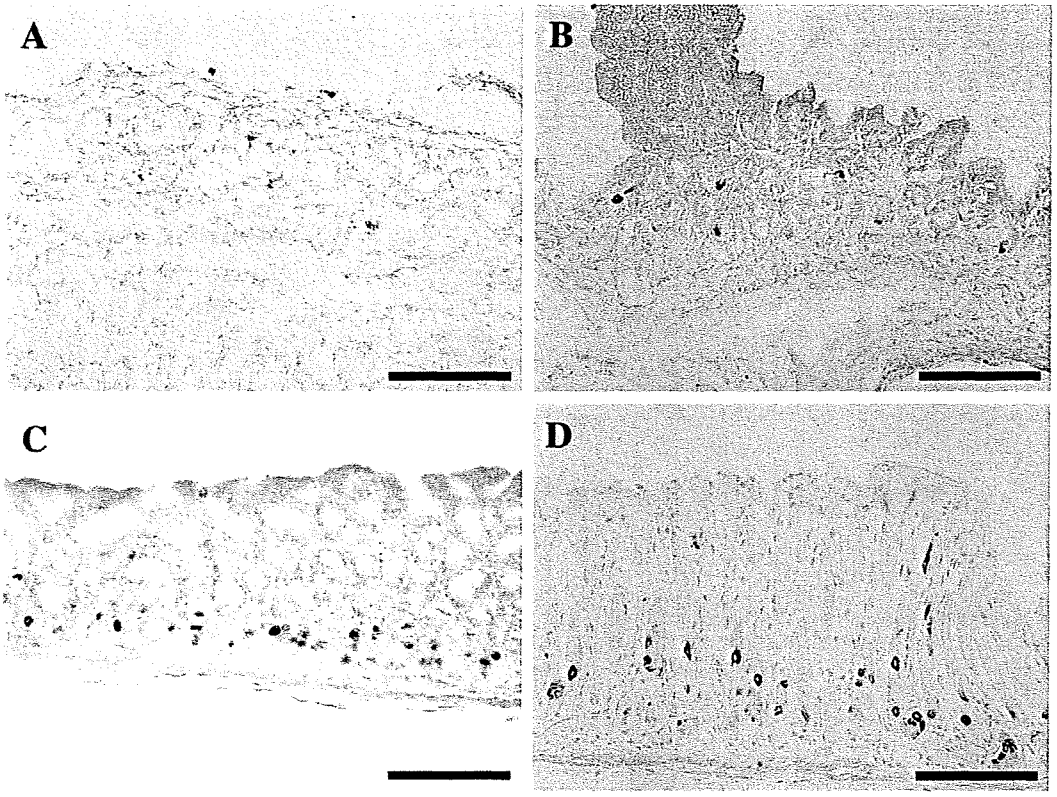

Fig. 2. Ontogeny of NPW-immunoreactive cells in the developing rat stomach. NPW-immunoreactive cells (*brown*) in the stomach of (A) postnatal day 1 of age, (B) postnatal day 7 of age, (C) postnatal day 21 of age, and (D) adult. The intensity of the staining increases during the progress of development. *Bars*, 100 μm in A–D. (For interpretation of the references to colour in this figure legend, the reader is referred to the web version of this article.)

P1. Thereafter, NPW mRNA slightly decreased through the end of weaning (P21) and then the level again increased two times through the progress of age until reaching adulthood.

3.2. NPW immunohistochemistry in the developing rat stomach

A few NPW cells are initially detectable in the postnatal P1 antral stomach (Fig. 2A). No NPW-immunoreactive cells were detectable in embryonic E14 and E17 stomach (data not shown). The density of NPW cells (*i.e.* number of NPW-containing cells/field) in the stomach increased progressively as a function of age until adulthood (Fig. 2B, C). Strongly stained NPW cells were present in the adult stomach (Fig. 2D). NPW-immunoreactive cells colocalized with gastrin cells in postnatal P1, P7, P21 and adult antral stomach (upper panel, Fig. 3). NPW-immunoreactive cells accounted for 57%, 54%, 60% and 85% of gastrin-immunoreactive endocrine cells in postnatal P1, P7, P21, and adult stomach, respectively (lower panel, Fig. 3). Gastrin cells were initially detectable in embryonic day E17 stomach (data not shown). No specific immunoreactivity was observed in the rat stomach when either normal rabbit serum or antiserum pre-absorbed with excessive NPW was used (data not shown).

4. Discussion

NPW was isolated from the porcine hypothalamus as a peptide ligand for the GPCRs, GPR7 and GPR8, using the cell-based reporter system [4]. Central administration of NPW augmented serum prolactin and corticosterone, suppressed dark-phase and fasting-induced feeding, and increased energy expenditure [6,7]. Chronic administration of NPW decreased food intake and produced weight loss [7]. These findings suggest that NPW may play a role in feeding behavior and energy homeostasis. In situ hybridization histochemistry has demonstrated expression of rat GPR7 mRNA and NPW mRNA in the stomach [9]. We have shown using immunohistochemistry that NPW-immunoreactive endocrine cells are present in the rat, mouse, and human stomach [10]. NPW-immunoreactive cells are abundant in the mucosal layer of the antrum in all three species. Three types of endocrine cells exist in the rat gastric antrum; gastrin cells, enterochromaffin (EC) cells, and D cells, which respectively secrete gastrin, serotonin, and somatostatin [13,14]. Using double immunohistochemistry and electron microscopic immunohistochemistry, we demonstrated that NPW cells are expressed with antral gastrin cells and more then 80% of NPW-immunoreactive cells were identifiable as antral gastrin cells [10]. NPW plasma concentration decreases upon fast and increased after refeeding in rats, suggesting that stomach NPW is involved in energy homeostasis [10]. The ontogeny of NPW in the developing rat stomach has yet to be clarified.

The present study showed that stomach NPW expression was detected early during development. NPW mRNA level was elevated in embryonic day E14 rat stomach and remained elevated until birth. Thereafter, NPW mRNA decreased slightly towards the end of the weaning period (P21). From the end of the weaning

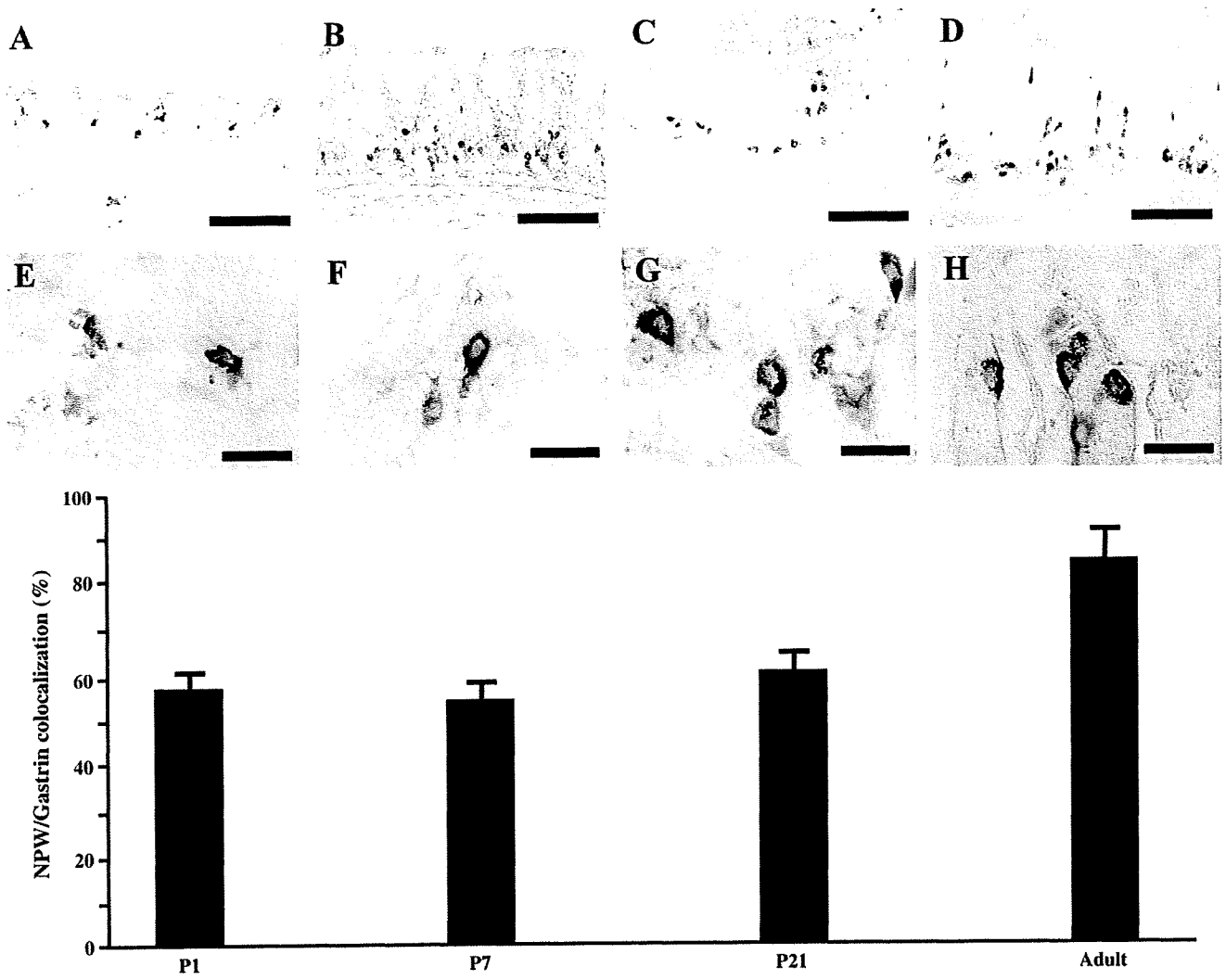

Fig. 3. Immunohistochemical localization of NPW in the developing rat stomach. Upper panel; NPW-immunoreactive cells (*brown*) colocalizes with gastrin (*blue-black*) in the stomach of (A) postnatal day 1 of age, (B) postnatal day 7 of age, (C) postnatal day 21 of age, and (D) adult. (E–H), Higher magnification of panel A–D. *Bars*, 100 μm in A–D and 20 μm in E–H. Lower panel; The percentage (%) of NPW cells colocalizing with gastrin cell in postnatal P1, P7, P21, and adult rat stomach, respectively. Values are mean±S.E., $n=3$. (For interpretation of the references to colour in this figure legend, the reader is referred to the web version of this article.)

period (P21) the NPW mRNA again increased two-fold with the progress of age until reaching adulthood. A few NPW-immunoreactive cells initially appeared in postnatal day 1 of age stomach. The NPW cells started to gradually increase in numbers during the second and third week of postnatal growth, reaching near-adult density after the weaning period. The discrepancy between NPW mRNA and NPW-immunoreactive cells after birth until weaning (P21) may be attributed to the low activity of the endocrine cells during this period [15]. After weaning the NPW-immunoreactive cells are more active as shown by the rapid rise in the NPW mRNA level. The observations that there is a developmental increase in NPW peptide in the stomach after weaning suggests that NPW may play an important role in the development of the GI tract.

Gastrin is a gut hormone which starts to appear in the rat stomach at embryonic day E17 of age and is of few numbers [15–18]. The gastrin cells remain few during the first postnatal week but start to increase in number during the second week, reaching near-adult density during weaning. In adult rats, the G cells are abundant in the antral mucosa where they may number $5\times10^5/cm^2$ [19]. At the time of birth and during the first two weeks after the birth, the pancreas represents an additional source of gastrin [20]. We previously showed that NPW cells colocalize with antral gastrin cells in the adult rat stomach [10]. Using double immunohistochemistry, we demonstrated that NPW colocalizes with gastrin cells in the developing rat stomach, starting from its initial presence in postnatal day 1 of age stomach. NPW colocalized with 57%, 54%, 60%, and 85% of gastrin in the postnatal P1, P7, P21, and adult rat stomach, respectively. The intensity of NPW cell staining increased during the developing stage. In the newborn rats, the serum gastrin concentration is low, which gradually increased until it peaked at about two to three weeks of age, the time of weaning [16–19]. The low serum gastrin concentration during the first two weeks after birth probably reflects the low number and/or low activity of the antral gastrin cells at this stage [16–19]. At

the time of weaning, the gastrin cells have reached a near-adult density and have become active, as reflected by the rise in the serum gastrin concentration. In the developing rat, gastrin is thought to be important for the maturation of the acid-producing (oxyntic) mucosa in general and for the development of ECL cells in particular [16]. The near-adult acid secretory capacity of the rat stomach is attained after the weaning period. In adult rats, gastrin stimulates acid secretion from the oxyntic cells and gastric motility. Gastrin also acts on the stem cells in the gastric glands to stimulate cell proliferation and differentiation. Taken together, the increased numbers of colocalization of NPW with gastrin indicate that NPW may play an important role in the development of the rat GI tract.

Interestingly, the developmental appearance of stomach NPW peptide differs from that of several other gut peptide such as apelin, ghrelin, and peptide YY. Apelin has been demonstrated in both gastric endocrine and exocrine cells [21]. The apelin mRNA expression is initially detectable at E16 of gestation and gradually increased during the progress of development, whereas its peptide expression is initially observed at weaning period (P21) and it increased progressively with age [21]. Ghrelin, which is found in the X/A-like cells of gastric fundus, is not detectable in the fetal rat stomach; however, ghrelin expression and peptide levels increase dramatically during the second and third postnatal weeks [12,22]. The developmental elevation in PYY occurs earlier than stomach ghrelin with PYY expression obvious in late gestation [23].

In summary, the present study demonstrated that NPW mRNA is initially expressed in embryonic day E14 of age rat stomach. NPW expression increased progressively with age until reaching adulthood. We also demonstrated that NPW cells were initially detected in postnatal day 1 of age stomach and the NPW cell numbers gradually increased during the progress of age. NPW colocalized with gastrin cells as early as postnatal day 1 of age stomach and the NPW cell staining intensity increased with the concurrent development. Previously we reported that plasma NPW concentration of the gastric antrum decreased significantly after 15-h fast and increased after refeeding in rats, suggesting that NPW acts as a catabolic signal in energy homeostasis [10]. The co-expression of NPW with gastrin and the ontogenic change of NPW in the developing rat stomach will help to clarify the physiological functions of this new enteric peptide, NPW.

Acknowledgements

This study was supported in part by the 21st Century COE Program and grants-in-aid from the Ministry of Education, Culture, Sports, Science, and Technology of Japan; the Ministry of Health, Labor, and Welfare of Japan; Takeda Science Foundation; Foundation for Growth Science; Smoking Research Foundation; Program for Strategic Regional Science and Technology Advancement; to M.N.

References

[1] O'Dowd BF, Scheideler MA, Nguyen T, Cheng R, Rasmussen JS, Marchese A, Zastawny R, Heng HH, Tsui LC, Shi X. The cloning and chromosomal mapping of two novel human opioid-somatostatin-like receptor genes, GPR7 and GPR8, expressed in discrete areas of the brain. Genomics 1995;28:84–91.

[2] Lee DK, Nguyen T, Porter CA, Cheng R, George SR, O'Dowd BF. Two related G protein-coupled receptors: the distribution of GPR7 in rat brain and the absence of GPR8 in rodents. Mol Brain Res 1995;71:96–103.

[3] Ishii M, Fei H, Friedman JM. Targeted disruption of GPR7, the endogenous receptor for neuropeptide B and W, leads to metabolic defects and adult-onset obesity. Proc Natl Acad Sci U S A 2003;100:10540–5.

[4] Shimomura Y, Harada M, Goto M, Sugo T, Matsumoto Y, Abe M, Watanabe T, Asami T, Kitada C, Mori M, Onda H, Fujino M. Identification of neuropeptide W as the endogenous ligand for orphan G-protein-coupled receptors GPR7 and GPR8. J Biol Chem 2002;277:35826–32.

[5] Kitamura Y, Tanaka H, Motoike T, Ishii M, Williams SC, Yanagisawa M, Sakurai T. Distribution of neuropeptide W immunoreactivity and mRNA in adult rat brain. Brain Res 2006;1093:123–34.

[6] Baker JR, Cardinal K, Bober C, Taylor MM, Samson WK. Neuropeptide W acts in brain to control prolactin, corticosterone, and growth hormone release. Endocrinology 2003;144:2816–21.

[7] Mondal MS, Yamaguchi H, Date Y, Shimbara T, Toshinai K, Shimomura Y, Mori M, Nakazato M. A role for neuropeptide W in the regulation of feeding behavior. Endocrinology 2003;144:4729–33.

[8] Fuji R, Yoshida H, Fukusumi S, Habata Y, Hosoya M, Kawamata Y, Yano T, Hinuma S, Kitada C, Asami T, Mori M, Fujisawa Y, Fujino M. Identification of a neuropeptide modified with bromine as an endogenous ligand for GPR7. J Biol Chem 2002;277:34010–16.

[9] Tanaka H, Yoshida T, Miyamoto N, Motoike T, Kurosu H, Shibata K, Yamanaka A, Williams SC, Richardson JA, Tsujino N, Garry MG, Lerner MR, King DS, O'Dowd BF, Sakurai T, Yanagisawa M. Characterization of a family of endogenous neuropeptide ligands for the G protein-coupled receptors GPR7 and GPR8. Proc Natl Acad Sci U S A 2003;100:6251–6.

[10] Mondal MS, Yamaguchi H, Date Y, Toshinai K, Kawagoe T, Tsuruta T, Kageyama H, Kawamura Y, Shioda S, Shimomura Y, Mori M, Nakazato M. Neuropeptide W is present in antral G cells of rat, mouse, and human stomach. J Endocrinol 2006;188:49–57.

[11] Chomczynski P, Sacchi N. Single-step method of RNA isolation by acid guanidinium thiocyanate-phenol-chloroform extraction. Ann Biochem 1987;162:156–9.

[12] Date Y, Kojima M, Hosoda H, Sawaguchi A, Mondal MS, Suganuma T, Matsukura S, Kangawa K, Nakazato M. Ghrelin, a novel growth hormone-releasing acylated peptide, is synthesized in a distinct endocrine cell type in the gastrointestinal tracts of rats and humans. Endocrinology 2000;141:4255–61.

[13] Solcia E, Capella C, Buffa R, Usellini L, Fiocca R, Sessa F. Endocrine cells of the digestive system. In: Johnson LR, editor. Physiology of the gastrointestinal tract. New York: Raven Press; 1987. p. 111–30.

[14] Walsh JH. Gastrointestinal hormones. In: Johnson LR, editor. Physiology of the gastrointestinal tract. New York: Raven Press; 1994. p. 1–128.

[15] Ekelund M, Hakanson R, Hedenbro J, Rehfeld JF, Sundler F. Endocrine cells and parietal cells in the stomach of the developing rat. Acta Physiol Scand 1985;124:483–97.

[16] Larsson LI, Hakanson R, Rehfeld JF, Stadil F, Sundler F. Occurrence and neonatal development of gastrin immunoreactivity in the digestive tract of the rat. Cell Tissue Res 1974;149:275–81.

[17] Bjorkqvist M, Dornonville de la Cour C, Zhao CM, Gagnemo-Persson R, Hakanson R, Norlen P. Role of gastrin in the development of gastric mucosa, ECL cells and A-like cells in newborn and young rats. Regul Pept 2002;108:73–82.

[18] Fawcett DW. The esophagus and stomach. In: Bloom W, Fawcett DW, editors. A textbook of histology. New York: Chapman and Hill; 1994. p. 605–15.

[19] Larsson LI, Rehfeld JF, Sundler F, Hakanson R. Pancreatic gastrin in foetal and neonatal rats. Nature 1976;262:609–10.

[20] Takeuchi K, Peitsch W, Johnson LR. Mucosal gastrin receptor. V. Development in newborn rats. Am J Physiol Gasterointest Liver Physiol 1981;240:G163–9.

[21] Wang G, Anini Y, Wei W, Qi X, OCarroll AM, Mochizuki T, Wang HQ, Hellmich MR, Englander EW, Greeley GH. Apelin, a new enteric peptide: localization in the gastrointestinal tract, ontogeny, and stimulation of

gastric cell proliferation and of cholecystokinin secretion. Endocrinology 2004;145:1342–8.

[22] Lee HM, Wang G, Englander EW, Kojima M, Greeley Jr GH. Ghrelin, a new gastrointestinal endocrine peptide that stimulates insulin secretion: enteric distribution, ontogeny, influence of endocrine, and dietary manipulations. Endocrinology 2002;143:185–90.

[23] Gomez G, Zhang T, Rajaraman S, Thakore KN, Yanaihara N, Townsend Jr CM, Thompson JC, Greeley GH. Intestinal peptide YY: ontogeny of gene expression in rat bowel and trophic actions on rat and mouse bowel. Am J Physiol Gasterointest Liver Physiol 1995;268:G71–81.

Use of ^{18}F-fluorodeoxyglucose-positron emission tomography to evaluate responses to neo-adjuvant chemotherapy for primary tumor and lymph node metastasis in esophageal squamous cell carcinoma

Tomoki Makino, MD,[a] Yuichiro Doki, MD,[a] Hiroshi Miyata, MD,[a] Takushi Yasuda, MD,[c] Makoto Yamasaki, MD,[a] Yoshiyuki Fujiwara, MD,[a] Shuji Takiguchi, MD,[a] Ichiro Higuchi, MD,[a] Jun Hatazawa, MD,[b] *and* **Morito Monden, MD,[a]** *Osaka, Japan*

Background. *Neoadjuvant chemotherapy (NACT) targets lymph node metastasis (LN), as well as the primary tumor (PT) in esophageal squamous cell carcinomas (ESCC). ^{18}F-fluorodeoxyglucose-positron emission tomography (FDG-PET) reflects viable tumor volume and may be more useful for evaluating NACT responses than conventional radiography. Moreover, FDG-PET may elucidate the clinical significance of NACT responses for LN, which is not always identical to those for PT.*

Patients and Methods. *We retrospectively investigated prognostic factors in 38 node-positive ESCC patients who had undergone NACT (5-fluorouracil, adriamycin, and cisplatin) and surgical resection. The NACT response was evaluated separately by both PET and computed tomography (CT) for each PT and LN.*

Results. *Although NACT effect for PT and LN was similar by PET evaluation (SUVmax reduction; average 70.58% vs 71.57%), they did not show significant correlation, revealing discordance for 13 (34.2%) patients when SUVmax reduction of more than 70% was classified as a PET responder. An opposite relationship existed in that the pre-NACT SUVmax of PT was significantly lower in PET responders than in PET non-responders (9.92 ± 4.3 vs 12.96 ± 3.8, P = .032), while that of LN tended to be higher in responders than in non-responders (5.70 ± 3.2 vs 3.77 ± 0.9, P = .072). Multivariate analysis identified the number of PET-positive LN (P = .018, HR = 5.464) and PET response for PT (P = .015, HR = 4.620) and for LN (P = .028, HR = 3.854) as independent prognostic predictors. The NACT response for PT or LN on CT evaluation was not a significant prognostic predictor.*

Conclusion. *PET is superior to CT for evaluating the NACT response from the viewpoint of survival analysis. The NACT response should be evaluated for both LN and PT because of their different behaviors during chemotherapy. Further studies of larger sample number should be conducted in the future. (Surgery 2008;144:793-802.)*

From the Department of Gastroenterological Surgery[a] and Department of Nuclear Medicine and Tracer Kinetics,[b] Graduate School of Medicine, Osaka University; and Department of Surgery, Kinki University,[c] Osaka, Japan

SURGICAL TREATMENT AND/OR RADIATION THERAPY have improved local control and short-term survival of esophageal cancers.[1-3] For the next step, adjuvant and/or neoadjuvant chemotherapy, aiming to control systemic micrometastasis, is expected to improve long-term survival. The presence of systemic micro-metastasis has been reported to be strongly associated with the presence of lymph node metastasis (LN),[4-6] which, unfortunately, can not be precisely evaluated by conventional radiographic examination. When systemic micrometastasis is present, response to chemotherapy is the most important factor influencing long-term survival.[5] Neoadjuvant chemotherapy (NACT), but not adjuvant chemotherapy, allows us to evaluate the chemotherapy

Accepted for publication June 21, 2008.

Reprint requests: Yuichiro Doki, MD, Department of Gastroenterological Surgery, Graduate School of Medicine, Osaka University, 2-2-E2, Yamada-oka, Suita, Osaka 565-0871, Japan. E-mail: ydoki@surg2.med.osaka-u.ac.jp.

0039-6060/$ - see front matter

doi:10.1016/j.surg.2008.06.026

response using various imaging modalities. Surgical treatment of this disease, ie, esophagectomy with lymph mode clearance via thoracotomy and reconstruction using abdominal tissue, involves one of the highest levels of physical invasiveness among digestive cancer surgeries. The operative indication therefore should be carefully decided based on long-term curability. To this end, there is a need to evaluate both the possibility of systemic micrometastases and the response to chemotherapy before surgery. However, this evaluation is very difficult using objective and non-invasive modalities.

^{18}F-fluorodeoxyglucose-positron emission tomography (FDG-PET) can detect small cancerous colonies with high specificity, and is now widely used to evaluate early tumors or small metastatic lesions in esophageal cancers.[7-11] FDG-PET has been reported to be useful for evaluating the response of chemoradiotherapy in locally advanced esophageal cancers,[12-15] probably because it is not affected by inflammation, edema, and fibrosis, and because it predominantly reflects the biological activity of the tumor. FDG-PET is thus clinically promising, although its use with respect to NACT of esophageal cancers remains largely unreported.

Proving the elimination of systemic micrometastasis by NACT has not been possible, even using imaging modalities such as CT, magnetic resonance imaging (MRI), ultrasonography and FDG-PET. An apparent decrease in size of the larger tumor, mostly represented by the primary tumor (PT), might be generally assumed to represent the disappearance of systemic micrometastases. However, cancer metastasis is a highly selective phenomenon and tumor characteristics differ greatly between primary and metastatic tumors.[16-19] Thus, evaluating the metastatic tumors rather than PT might enable more precise indications of the elimination of micrometastases by NACT. Although LN is generally smaller than PT in esophageal cancers, the specificity of FDG-PET may differentiate small changes in LN by NACT. The present study investigated the value of FDG-PET in evaluating NACT effects on node-positive esophageal cancers, by associating various tumor parameters with postoperative survival. We discuss how FDG-PET can impact on the treatment strategy for esophageal cancers treated by NACT.

MATERIALS AND METHODS

Background patient data. From 2001 to 2005, 251 patients with esophageal squamous cell carcinoma (ESCC) were admitted and treated in our department. All underwent esophageal fiberscopy, esophagography, and enhanced CT imaging from neck to abdomen for tumor staging according to the TNM classification.[20] Some patients also underwent MRI, endoscopic ultrasonography, or bronchial fiberscopy to obtain further information. Our strategy for ESCC based on TMN classification was as follows: preoperative chemoradiotherapy for cT4N0M0, NACT for cTanyN1M0, and surgery without preoperative treatment for cT1-T3N0M0. This strategy is based on the importance of local control in cT4N0M0, and eradication of systemic spread and hence improvement of prognosis of patients with cTanyN1M0 tumors. Patients with distant metastases were not indicated for radical esophagectomy. In total, 63 patients received NACT with informed consent. Among these, 12 did not undergo FDG-PET pre- and/or postoperatively, four showed no surgical indication after NACT, and nine were LN-positive by CT imaging, but negative by FDG-PET. After these patient exclusions, 38 patients were enrolled in the final retrospective study.

There were 7 female and 31 male patients with a mean age of 62.3 years (range 50–76 years). Table I details the patient characteristics. All 38 patients received the same regimen of NACT (5-fluorouracil + adriamycin + cisplatin) and subsequent surgical resection. Imaging by FDG-PET and CT was conducted on all patients both pre-NACT (within 2 weeks of the first administration) and post-NACT (2–3 weeks after the last administration).

Table I. Patient characteristics (n = 38)

Parameters	*Classification*	*Number of patients*
Age (year)		62.3 (50–76)*
Gender	male/female	31/7
Histology	well/mod/poor†	7/18/13
Location	upper/middle/lower	8/16/14
cT‡	0/1/2/3/4	0/2/11/21/4
pT	0/1/2/3/4	2/9/7/14/6
cN	N1/M1lym	15/23
pN	N0/N1/M1lym	11/12/15
Number of pN	0/1–3/4–7/8–	10/11/7/10
Number of cN by PET§	1–3/4–	26/12
cStage‖	0/I/II/III/IV	0/0/4/11/23
pStage‖	0/I/II/III/IV	2/3/9/9/15

*Average and range.
†Well, moderately and poorly differentiated squamous cell carcinoma.
‡cT, cN, cStage (clinical classification) pN, pT, pStage (pathological classification) and M1lym (distant lymph node metastasis) are according to TNM classification.
§Number of PET positive lymph nodes before neo-adjuvant therapy
‖cStage: clinical stage before neoadjuvant chemotherapy; pStage: pathological stage determined by histopathological examination of the surgically resected specimen after chemotherapy.

After NACT, 34 patients (89.5%) underwent curative resection (R0), while non-curative resection (R2) was done for 4 patients (10.5%) who were excluded from the survival analysis. Patients were surveyed postoperatively every 3 months by physical examination and serum tumor markers, every 6 months by CT scan and abdominal ultrasonography, and every year by endoscopy until tumor recurrence was evident. Postoperative chemotherapy or radiotherapy was not routinely performed. Patients with tumor recurrence after surgery received taxan-based chemotherapy if tolerable for their systemic condition. The median overall survival was 20.5 months and median disease-free survival was 10.7 months. The median follow-up period after surgery was 31.2 months.

Neoadjuvant chemotherapy and surgical treatment. To receive NACT, patients had to satisfy clinical criteria including an Eastern Cooperative Oncology Group performance status of 0 to 1 and normal function of the bone marrow, kidney, and liver. The regimen consisted of 2 courses of 5-fluorouracil (5-FU), cisplatin (CDDP), and adriamycin (ADM).[5,21,22] The chemotherapy dosage was as follows. CDDP (70 mg/m^2) and ADM (30 mg/m^2) were given intravenously for 2 hours on day 1 and 5-FU (700 mg/m^2) was administered by continuous intravenous infusion on day 1 to 7. This course was repeated twice every 28 days unless patients showed progressive disease after one course of chemotherapy. Three patients received a 30% dose reduction at the second cycle because of grade 3 or more toxicity assessed by NCI-CTC criteria[23] in the first cycle. Thirty-three patients (86.8%) received 2 courses of NACT and five (13.2%) had only one course, due to renal dysfunction that appeared after chemotherapy in 1 patient and the refusal of 2 patients to continue due to severe symptoms, and to apparent tumor growth during the first course observed in 2 patients.

Surgical therapy consisted of en bloc esophagectomy via right thoracotomy and reconstruction with a gastric tube.[4] Three-field lymphadenectomy was performed for 23 patients (60.5%) with upper-third thoracic esophageal carcinoma or with metastasis in the upper mediastinal and/or cervical lymph nodes. The remaining patients received 2-field lymphadenectomy.[24] No patients died of post-operative complications, although postoperative morbidity was observed in 12 patients (31.6%), including pulmonary complications (6 patients), anastomotic leakage (4 patients), and transient recurrent nerve paralysis (3 patients).

Tumor evaluation by PET and CT. PET was performed according to a previously described protocol.[25-27] All patients fasted for at least 4 hours before the PET scanning. Blood glucose levels were measured just before FDG injection and confirmed to be less than 150 mg/dl. For each PET scan patients received an intravenous injection of approximately 370 MBq FDG. Simultaneous emission-transmission PET scans were acquired 1 hour after FDG injection (transmission source: 68Ge-68Ga line source). FDG-PET was performed with a dedicated PET scanner (HEADTOME/SET 2400W; Shimadzu, Kyoto, Japan), which has 32 rings of bismuth germanate detectors and simultaneously produces 63 slices of 3.125 mm thickness along a 20-cm longitudinal field. The intrinsic resolution was 3.7 mm full width at half-maximum, and the sensitivity of the device was 7.3 cps/Bq/cm3. Scans required 4 bed positions to cover the area from the neck to the pelvis, each with an acquisition time of 10 minutes, resulting in a total scanning time of 40 minutes. Images were reconstructed with an iterative median root prior to using a reconstruction algorithm (mask size 3 × 3, β0.3, subsets 24, iteration 1).

Transaxial, coronal, and sagittal image sets were displayed on a high-resolution monitor as a linear gray scale. For semi-quantitative analysis, regions of interests (ROIs) (diameter of 1.5 cm, corresponding to 10 pixels) were placed over the PT or LN in the slice with maximum FDG uptake on baseline scan. The maximal standardized uptake value (SUVmax) was then calculated, according to the following formula: PET count of the most intense point × calibration factor (MBq/kg)/body weight (kg). In this study, we used SUVmax, which showed high reproducibility, but not SUVmean, which is easily affected by demarcation of ROI. The FDG uptake of the tumor is visible when the SUVmax exceeds approximately 2.0. In the present study, patients showing 2.0 or more SUVmax in LN were judged as PET-positive. When there was no FDG uptake, the fusion images combined with PET images and CT images were composed by our previously described method[25-27] and SUVmax was calculated by drawing ROIs on the area corresponding to PT or LN. We measured SUVmax of PT and LN both pre- and post-NACT as the response evaluation in PET diagnosis. Next, we calculated SUVmax reduction by subtracting background SUVmax (1.752), which was the mean value of our present cases. When more than 2 PET-positive LNs existed, the one the highest SUVmax was used for the response evaluation, because it was the least affected by the background, and the response rate was similar among several positive LNs in the same patient.

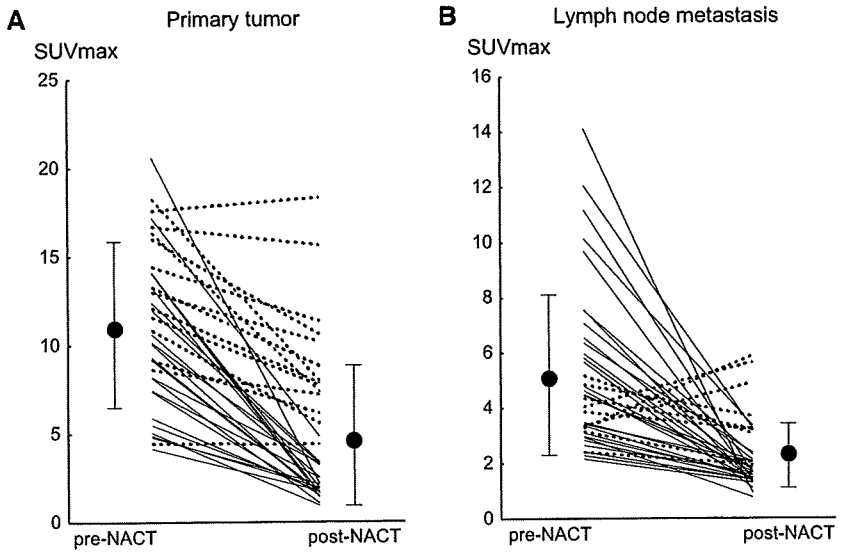

Fig 1. Change of SUVmax before and after neoadjuvant chemotherapy of primary tumor and lymph node metastasis. SUVmax before and after neoadjuvant chemotherapy (NACT) are shown in each patient for the primary tumor (*A*) and lymph node metastasis (*B*). Straight line and dotted line show responders and nonresponders respectively. Average and standard deviation of each group are indicated with closed circles and bars. Primary tumor; pre-NACT (11.12 ± 4.32) and post-NACT (4.83 ± 4.18) and lymph node metastasis pre-NACT (5.19 ± 2.92) and post-NACT (2.22 ± 1.21).

For CT diagnosis, we measured maximal tumor areas in pre- and post-NACT scans using a 64-channel multi-detector CT, which allowed reconstruction using 0.625 mm slices, and calculated the decrease rate of the PT and LN areas. Rather than using a single measurement of the longest diameter as a RESICT criterion, we used 2-directional measurement for evaluation because primary esophageal cancers are frequently oval or irregularly shaped. When more than 2 LNs were observed on the CT or PET scan, we used the LN with the largest area for response evaluation, which was always equivalent to the one with the highest SUVmax.

Statistical analysis. Differences in continuous values of SUVmax were evaluated by the Student *t* test between the 2 groups. The association between 2 non-continuous parameters was evaluated by the Mann-Whitney *U* test, the chi-square test, and the Fisher exact test. Regression analysis was used to determine the correlation between SUVmax and tumor areas or between SUVmax of PT and LN showing Pearson's correlation coefficient (R value). Prognostic variables were assessed by log-rank test, and disease-free survival was analyzed by the Kaplan-Meier method. Cox's proportional hazard regression model with stepwise comparisons was used to analyze the independent prognostic factor. These analyses were carried out using StatView J 5.0 software statistical package (Abacus Concepts, Berkeley, Calif). Data are expressed as mean ± SEM. A P value less than .05 was considered statistically significant.

RESULTS

Tumor status and effect of NACT evaluated by FDG-PET and CT scan. The mean SUVmax value of PT before NACT was 11.12 ± 4.32, and correlated with tumor area (R^2 = 0.223, P = .003) and depth of tumor invasion (P = .03). However, there was no correlation with other clinico-pathological parameters including histological differentiation, location, age, and sex (data not shown). PET imaging detected a positive LN average of 2.45 per patient (1 to 5) before NACT (Table I). The mean SUVmax value of LN, represented by the LN with the highest SUVmax, was 5.19 ± 2.92, which also positively correlated with the tumor area of LN by CT scan (R^2 = 0.444, P < .0001). There were no significant correlations between pre-SUVmax values of PT and LN (R = 0.002, R^2: not available, P = .989).

After NACT, the mean SUVmax values of PT and LN were 4.83 ± 4.18 and 2.22 ± 1.21, respectively (Fig 1). Both PT and LN showed significant SUVmax reduction compared to values before NACT (P < .0001). The reduction rate, for which background SUV (1.752) was subtracted, was similar for PT and LN (70.58 ± 33.06 % and 71.57 ± 59.08%, respectively). According to the mean SUVmax reduction rate, patients with a

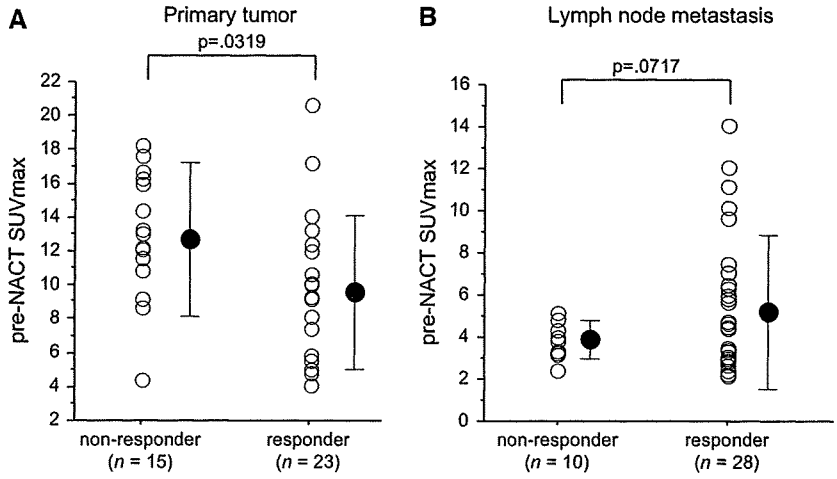

Fig 2. Relationship between NACT effect evaluated by PET and pre-NACT SUVmax in the primary tumor and lymph node metastasis. SUVmax before NACT is shown separately for the PET non-responder (SUVmax reduction <70%) and PET responder (≥70%) for the primary tumor (*A*) and lymph node metastasis (*B*). Average and standard deviation of each group are indicated with closed circles and bars. Non-responder for primary tumor showed significantly higher SUVmax before NACT than responder (12.96 ± 3.78 vs 9.92 ± 4.30, $P = .032$), while that for lymph node metastasis tended to show lower SUVmax before NACT than the counterpart (3.77 ± 0.85 vs 5.70 ± 3.23, $P = .072$).

rate of ≥70% were defined as PET responders and the remainder as non-responders for PT and LN. Using this cut-off value (70%), the difference in survival between responders and non-responders was significantly the highest for both PT and LN. When the response to NACT for PT and LN was compared using this cutoff value, 19 (50%) patients were classified as responders for both PT and LN, while 6 (15.8%) were non-responders for both. However, 13 (34.2%) patients showed discordant responses for PT and LN, including 9 LN responders who were PT non-responders and 4 PT responders who were LN non-responders. There was no significant correlation between the response evaluations of NACT for PT and LN ($P = .15$).

We compared the NACT responses for PT and LN with the pre-NACT clinico-pathological factors, including sex, age, location, histology, location of metastatic lymph node and tumor stage, but found no significant correlation among them (data not shown). There was a significant inverse correlation between SUVmax reduction rate and pre-NACT SUVmax for PT; PET responders showed significantly lower pre-NACT SUVmax than PET non-responders (9.92 ± 4.30 vs 12.96 ± 3.78, $P = .032$) (Fig 2). Interestingly, an opposite relationship of PET response with pre-NACT SUVmax was observed between PT and LN. That means PET responders showed higher pre-NACT SUVmax than non-responders for LN, although this difference was statistically marginal (5.70 ± 3.23 vs 3.77 ± 0.85, $P = .072$) (Fig 2). Since SUVmax was well correlated with tumor area measured by CT for both PT and LN, PET response showed the similar relationship with the pre-NACT tumor area. PET responders showed a significantly smaller pre-NACT tumor area than PET non-responders for PT (716.6 ± 597.3 mm^2 vs 1055.4 ± 511.1 mm^2, $P = .007$), while pre-NACT tumor area was not different significantly between PET responders and non-responders for LN (384.1 ± 505.8 mm^2 vs 294.5 ± 400.7 mm^2, $P = .371$).

Conventional CT evaluation based on 2-directional measurement produced a mean decrease rate for the PT and LN areas of 53.45 ± 28.39% and 47.01 ± 26.98%, respectively. There was a significant correlation between NACT response evaluated by SUVmax reduction (cut off, 70%) and decrease rate of tumor area (cutoff, 50%), both for PT ($P = .0002$) and LN ($P = .003$). Similar to the PET response, the CT response for PT and LN did not correlate each other ($P = .188$), nor associated with clinico-pathological factors (data not shown).

Survival. Disease recurrence after complete resection (R0) was diagnosed in 17 (50%) of the 34 patients. The mean time to recurrence was 21.4 months and the total 2-year disease-free survival (2-DFS) rate was 48.7%. Common parameters obtained before NACT including, age, sex, location, histology, tumor depth, distant lymph node metastasis (cM1lym), and pre-NACT tumor area did not correlate with survival (Table II), while some of the PET parameters before NACT including SUVmax of PT (<12) and the number of PET-positive LN

Table II. Univariate survival analysis of disease-free survival by Cox's proportional hazard model

	Number of cases	*HR*	*95% CI*	P
Location (Mt, Lt/Ut)*	28/6	1.613	0.525–4.955	.404
Histology (well, mod/por) †	23/11	1.919	0.197–1.376	.188
Pre-NACT SUVmax of PT (<12/≥12)	18/16	2.812	1.035–7.642	.044
Number of cN by PET(<4/≥4)	24/10	2.801	1.067–7.353	.037
SUVmax reduction in PT (≥70%/<70%)	21/13	3.906	1.476–10.335	.006
SUVmax reduction in LN (≥70%/<70%)	25/9	2.753	1.001–7.570	.05
Decrease of PT area (≥50%/<50%)	18/16	2.557	0.943–6.931	.065
Decrease of LN area (≥50%/<50%)	18/16	1.946	0.738–5.130	.178
pT (T1,2/T3,4)	18/16	4.064	1.412–11.699	.009
Number of pN(<4/≥4)	21/13	3.759	0.097–0.730	.010
Pathological response (1b 2 3/0 1a)	14/20	3.053	0.994–9.382	.051

HR, Hazard ratio; *CI*, confidence interval; *NACT*, neo-adjuvant chemotherapy; *PT*, primary tumor; *LN*, lymph node metastasis.
*Mt, Lt, Ut: middle, lower, and upper thoracic esophagus.
†Histology, pT, and pN are according to TNM classification.

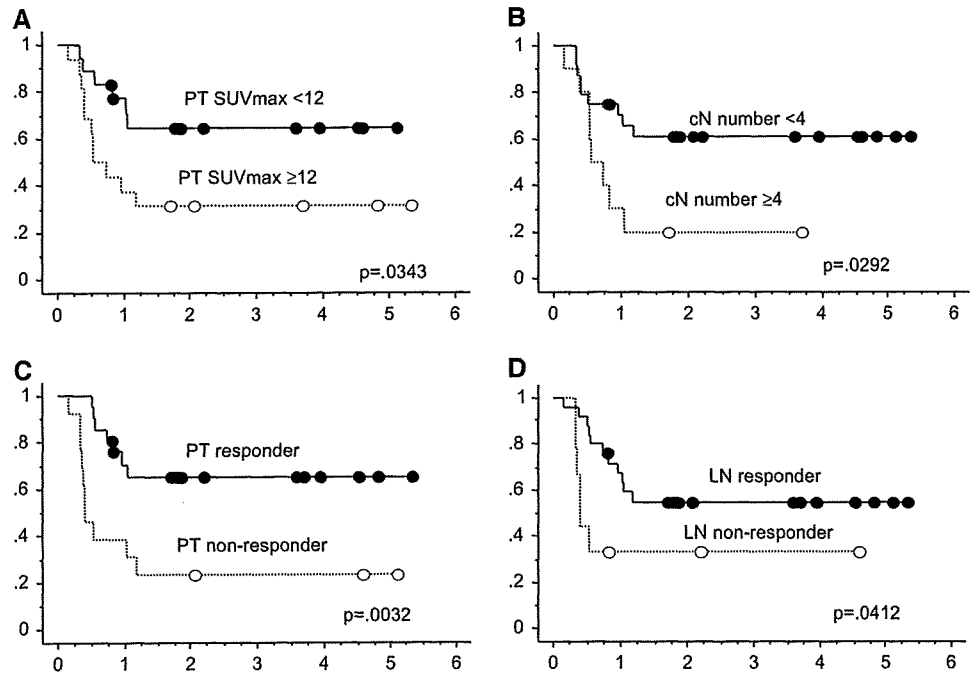

Fig 3. Survival curves of node-positive esophageal cancer patients who underwent NACT classified by various prognostic factors. Disease-free survival curves of node positive esophageal cancer patients who underwent NACT and curative resection were plotted by Kaplan-Meier methods. They were classified by various prognostic factors, including SUVmax of PT before NACT (*A*), number of cN evaluated by PET (*B*), PET response for PT (*C*) and LN (*D*). The difference of the two groups was evaluated by log rank test. Vertical and horizontal values indicate disease-free survival rate and year after surgery.

(<4) showed better 2-DFS than their counterparts (64.5% vs 31.3%, $P = .034$, and 60.9% vs 20.0%, $P = .029$, respectively) (Fig 3). With respect to post-NACT factors, PET responders (SUVmax reduction ≥70%) in PT and LN had better 2-DFS than non-responders (65.1% vs 23.1%, $P = .003$, and 54.9% vs 33.3%, $P = .041$, respectively) (Fig 3). In contrast, CT responders (decrease rate of tumor area ≥50%) in either PT or LN showed no significant survival benefit (Table II). A favorable prognosis was significantly associated with pathological factors after surgery, less tumor invasion (pT1, 2), and fewer

Table III. Multivariate survival analysis of disease-free survival by Cox's proportional hazard model

	Model 1†			*Model 2*		
*Parameters**	*HR*	*95% CI*	P	*HR*	*95% CI*	P
Pre-NACT SUVmax of PT	1.918	0.646–5.691	.240	1.497	0.489–4.583	.48
Number of cN by PET	6.757	1.838–25.000	.004	5.464	1.333–22.222	.018
SUVmax reduction in PT	5.993	1.882–19.092	.002	4.620	1.354–15.760	.015
SUVmax reduction in LN	3.987	1.249–12.726	.02	3.854	1.155–12.853	.028
pT	NI†			2.162	0.642–7.276	.213
Number of pN	NI			1.898	0.589–6.135	.2831

NI, Not included in the analysis.
*Classification, number of each category, abbreviations are given in Table I.
†Multivariate analyses with significant parameters obtained after NACT (model 1) and after surgery (model 2).

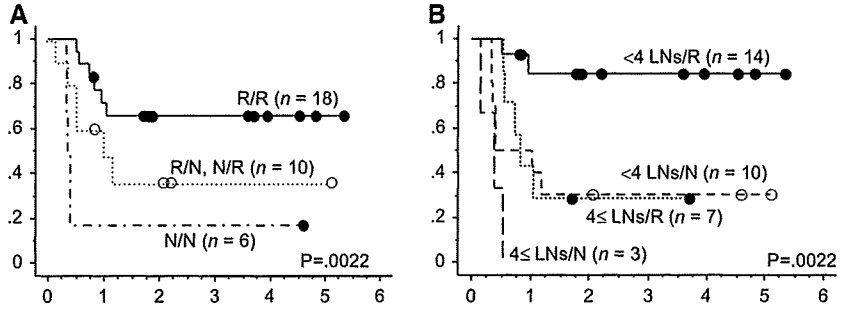

Fig 4. Survival curves according to significant prognostic factors. Disease-free survival curves of node-positive esophageal cancer patients who underwent NACT and curative resection were plotted by Kaplan Meier methods. Patients were subclassified according to the prognostic factors identified by multivariate analysis (see Table 4); (*A*) PET response in PT and LN, and (*B*) number of PET-positive LN and PET response in PT. R/R: PET responders for both PT and LN , N/R responders for either PT and LN and N/N nonresponders for both PT and LN. Difference between groups was evaluated by log rank test.

(<4) pathological lymph node metastases (2-DFS rate; 71.8% vs 21.9% $P = .005$, 66.7% vs 11.5% $P = .006$, respectively). Pathological evaluation of the response to NACT tended to be associated with DFS, but this trend was not statistically significant ($P = .051$) (Table II).

Univariate survival analysis using Cox's proportional hazard model identified the following significant prognostic factors: pre-NACT SUVmax of PT, pre-NACT number of PET-positive LN, SUVmax reduction of PT and LN, pathological T stage, and number of pathologically positive LN (Table II). Multivariate analysis using the pre-surgery factors identified the pre-NACT number of PET-positive LN and SUVmax reduction of PT and LN as significant independent prognostic factors (HR = 6.757 $P = .004$, HR = 5.993 $P = .002$, and HR = 3.987, $P = .02$, respectively) (Table III). These 3 parameters were also identified as the only significant independent prognostic factors when the multivariate analysis included post-surgery pathological factors, in addition to the pre-surgery factors (HR = 5.464, $P = .018$, HR = 4.620, $P = .015$, and HR = 3.854, $P = .028$, respectively) (Table III). For further analysis, we selected fewer parameters for multivariate analysis. When the above 3 parameters (number of PET-positive LN and SUVmax reductions of PT and LN) or each two of them ([number of PET-positive LN and SUVmax reduction of PT] and [number of PET-positive LN and SUVmax reduction of LN]) were entered in the multivariate analysis, the parameters selected were identified as independent prognostic factors. In order to understand these relationships, we separated the survival curves by the subclassification of each two of these parameters. Fig 4 showed the trend that prognosis was affected by both PET response in PT and LN and number of PET-positive LN and PET response in PT.

DISCUSSION

Our results indicated that FDG-PET is a superior modality to CT for survival prediction in esophageal cancer patients who underwent

NACT and subsequent surgery. This finding is consistent with previous reports of esophageal cancers treated by chemo-radiotherapy,[12-15] in which reduction of the PT was more accurately estimated by FDG-PET than by CT scan. The present study identified two other parameters determined by PET to be independent prognostic factors, namely the number of LN and the NACT effect for LN. These two prognostic factors offer new insights not only because they were obtained by FDG-PET, but also because they were consistent with the principle of NACT.

In this study, the response evaluation by CT did not correlate with survival. One possible reason is that NACT may induce inflammatory reactions associated with edema or scar tissue, and these may mask changes in tumor tissue volume on CT.[28,29] Secondly, morphological evaluations of digestive tract cancers are difficult because they do not form a solid tumor, but rather spread through the lumen. CT was also inadequate for evaluating small tumors, which generally show little size alteration due to NACT. In contrast, since FDG is selectively incorporated into viable tumor cells, the SUVmax value in the FDG-PET examination was seldom affected by either inflammation or morphological changes in form and/or size.[12-15] Another benefit of small-tumor evaluation by FDG-PET is the ability to eliminate the influence of normal structures, such as esophageal wall or lymph node, by subtracting the background SUV as performed in the present study. However, we should consider that small metastatic LN in many ESCC patients were probably not detected either by CT or PET and evaluation of small tumors might include accidental error even using PET.

One of the main objectives of NACT is to eradicate micrometastases, and the number of PET-positive LN before NACT might predict their presence. PET has poorer sensitivity for detecting positive LN than CT, but is far superior in specificity, thus PET offers higher overall accuracy than CT.[7,11,30,31] The present study showed that patients with numerous positive LN clinically showed poor prognosis despite receiving NACT followed by surgery. However, this does not suggest that these patients should be treated by other modalities, including surgery or chemoradiation. We should rather recognize that they should have received the benefit of NACT, because systemic chemotherapy is the only procedure available for eradicating systemic micrometastases and reducing advanced esophageal cancer from a systemic disease to a locoregional one. For example, a recent study (JCOG9204[32]) revealed the clinical benefit of adjuvant chemotherapy only for node-positive patients and not for node-negative patients, although the overall prognosis was poorer in the former. Based on this observation, node-positive patients were indicated for NACT in our institution. However, we should consider that the more positive LN present, the greater the chemotherapeutic effect needed to obtain good prognosis. It was probably encouraging that SUVmax reduction in patients with several metastatic LNs (reduction rate: 68% for >4 LN) was not worse than that of patients with fewer metastatic LN (reduction rate: 78% for <4 LN, $P = .73$). We need to examine more cases to draw definite conclusions on this issue.

When micrometastasis, for example in the lymph nodes, exists, its eradication by NACT would correlates with a reduction in macroscopic-sized tumors. We recently reported this relationship by investigating lymph node micrometastasis with cytokeratin immunohistochemistry; lymph node micrometastasis, which was a poor prognostic factor, was less frequent in patients given NACT than in those not given it, especially in those with a good response to NACT.[5] Consistent with this, many clinical trials showed a good response to chemotherapy or chemoradiotherapy closely associated with favorable prognosis.[33-35] Furthermore, the present study focused on the difference in NACT response between PT and LN and the associated clinical significance. We found that the NACT effect observed as SUVmax reduction was totally equivalent in PT and LN, although it frequently showed individual variations, and that these effects are independent prognostic factors. This might suggest PT and LN are not merely tumors at two different anatomical sites derived from the same origin, but have different biological and clinical properties. Of great interest is our finding of an opposite relationship in NACT response and pre-NACT SUVmax between PT and LN; responders for PT tended to have a small pre-NACT SUVmax, while those for LN a large pre-NACT SUVmax. This is consistent with observations that larger esophageal cancers tended to be more chemoresistant in the previous study[22,36] and that the pre-NACT SUVmax was significantly correlated with tumor size measured by CT in this study. It is speculated that large-size tumors are often heterogeneous in tumor clonality and microenvironment,[37] such as drug delivery, hypoxia, and immunity, and thus more resistant to chemotherapy. On the other hand, we found LN to show the following characteristics in this study: the mean LN size was smaller than PT size, the